Dynes Superconductors Theory Cornerstones

The effect of disorder in real-life superconductive samples experiments

František Herman

Dynes Superconductor
Original motivation

Tunneling conductance of MoC films, $T \approx 0.5K$

→ *Fits to Dynes formula*

→ $\bar{\Delta} \gtrsim \Gamma$

→ *Γ does not vanish at low temperature (elastic processes)*

→ *frequently observed (generic mechanism)*

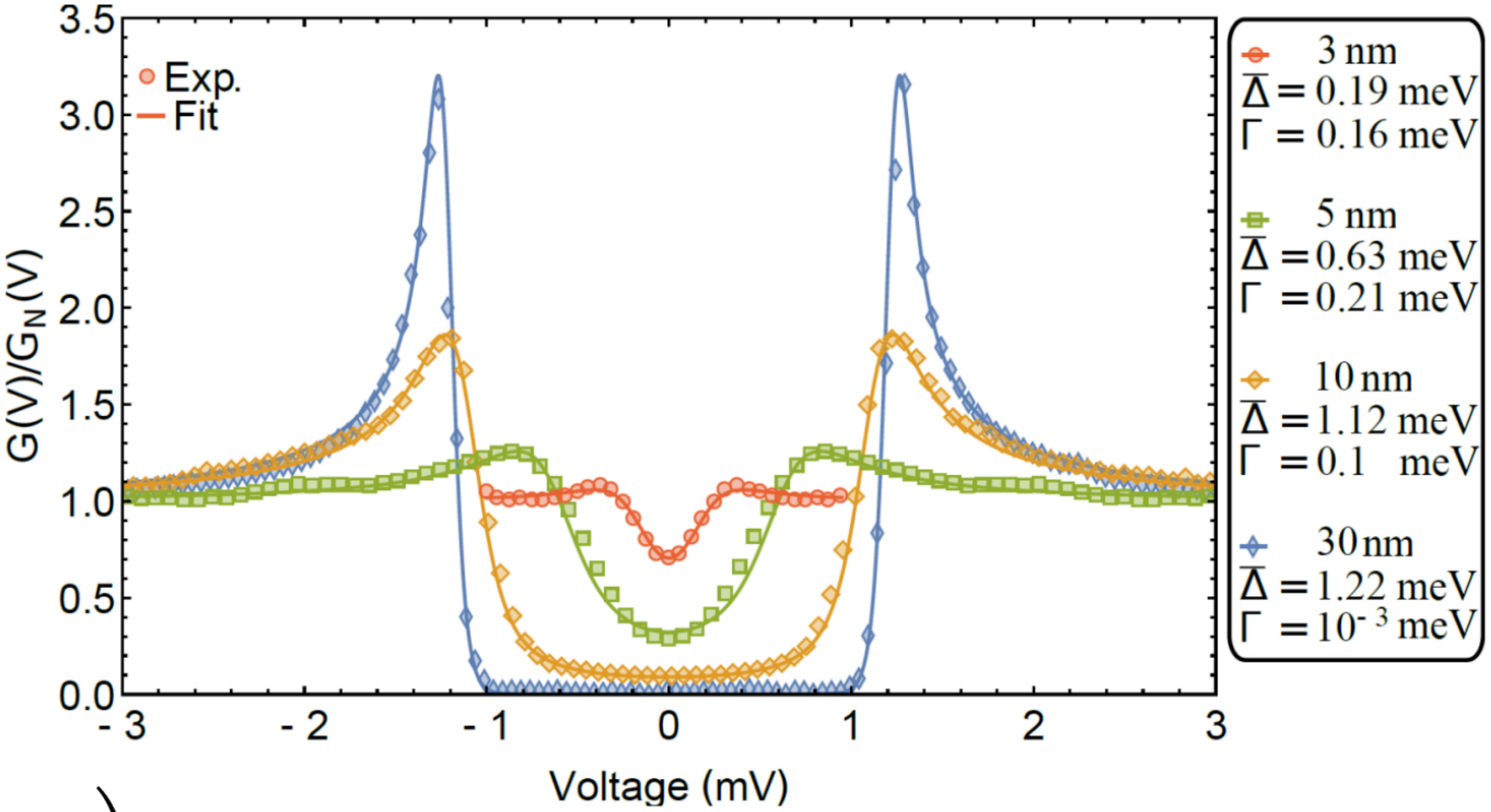

$$N(\omega) = N_0 \mathrm{Re}\left(\frac{\omega + i\Gamma}{\sqrt{(\omega + i\Gamma)^2 - \Delta^2}}\right)$$

Szabó *et* al., PRB **93**, 014505 (2016)

Green Function method

In the superconductive state

$$G_R(\boldsymbol{k}, t - t') = -i\langle\{c_{\boldsymbol{k}}(t) c_{\boldsymbol{k}}{}^{+}(t')\}\rangle\Theta(t - t')$$

$$\langle X\rangle = Tr\left(X\frac{e^{-H/T}}{Z}\right)$$

$$G(k, \omega_n) = \frac{1}{i\omega_n - \varepsilon_{\boldsymbol{k}}}$$

$$G(\mathbf{k}, \tau) = \begin{pmatrix} -\langle T c_{\mathbf{k}\uparrow}(\tau) c^{\dagger}_{\mathbf{k}\uparrow}\rangle & -\langle T c_{\mathbf{k}\uparrow}(\tau) c_{-\mathbf{k}\downarrow}\rangle \\ -\langle T c^{\dagger}_{-\mathbf{k}\downarrow}(\tau) c^{\dagger}_{\mathbf{k}\uparrow}\rangle & -\langle T c^{\dagger}_{-\mathbf{k}\uparrow}(\tau) c_{-\mathbf{k}\downarrow}\rangle \end{pmatrix}$$

Green Function method

In the superconductive state

$$G_R(\boldsymbol{k}, t-t') = -i\langle\{c_{\boldsymbol{k}}(t)c_{\boldsymbol{k}}^{+}(t')\}\rangle\Theta(t-t')$$

$$\langle X\rangle = Tr\left(X\frac{e^{-H/T}}{Z}\right)$$

$$G(k,\omega_n) = \frac{1}{i\omega_n - \varepsilon_{\boldsymbol{k}}}$$

$$G(\mathbf{k},\tau) = \begin{pmatrix} -\langle Tc_{\mathbf{k}\uparrow}(\tau)c^{\dagger}_{\mathbf{k}\uparrow}\rangle & -\langle Tc_{\mathbf{k}\uparrow}(\tau)c_{-\mathbf{k}\downarrow}\rangle \\ -\langle Tc^{\dagger}_{-\mathbf{k}\downarrow}(\tau)c^{\dagger}_{\mathbf{k}\uparrow}\rangle & -\langle Tc^{\dagger}_{-\mathbf{k}\uparrow}(\tau)c_{-\mathbf{k}\downarrow}\rangle \end{pmatrix}$$

- Main object: *Nambu-Gorkov averaged Green's function* $\hat{G}_M$, defined by: $\hat{G}_M^{-1} = \hat{G}_0^{-1} - \hat{\Sigma}$.

i) $\hat{G}_0^{-1}(\mathbf{k},\omega_n) = i\omega_n\tau_0 - \varepsilon_{\mathbf{k}}\tau_3$: the bare Green's function.

ω_n: Matsubara frequencies, τ_i: Pauli matrices.

ii) $\hat{\Sigma}_n = i\omega_n(1-Z_n)\tau_0 + Z_n\Delta_n\tau_1$: *Self-energy* generated by disorder and pairing interactions. Functions Δ_n and Z_n contain complete information about the properties of the considered superconductor.

Coherent Potential Approximation

Soven, Velický et. al., Weinkauf and Zittart 75

T- matrix approx. (perturbative approach → Feynman diagrams):

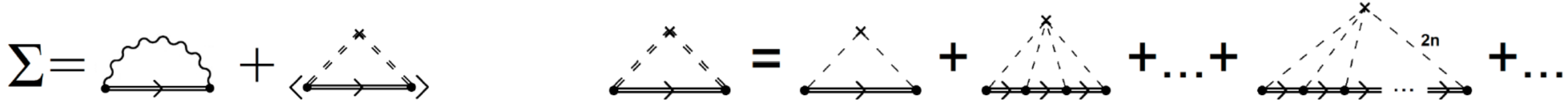

*CPA (**non**perturbative approach → self-consistent theory):*

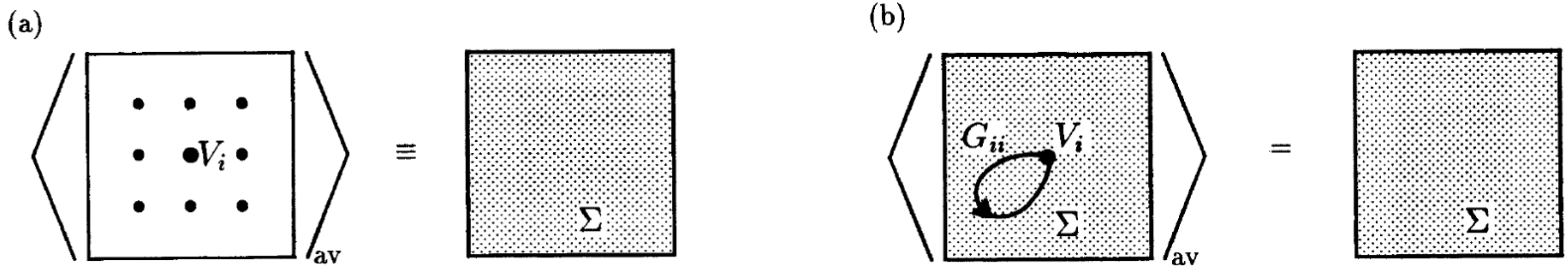

$$\hat{\mathcal{G}}_n = \frac{1}{N}\sum_{\mathbf{k}} \hat{G}(n\mathbf{k}), \qquad \hat{\mathcal{G}}_n = \left\langle \left(\hat{\mathcal{G}}_n^{-1} - \hat{V} + \hat{\Sigma}_n \right)^{-1} \right\rangle$$

TMA vs. CPA

ξ: *superconducting coherence length*

l: *characteristic distance between impurities*

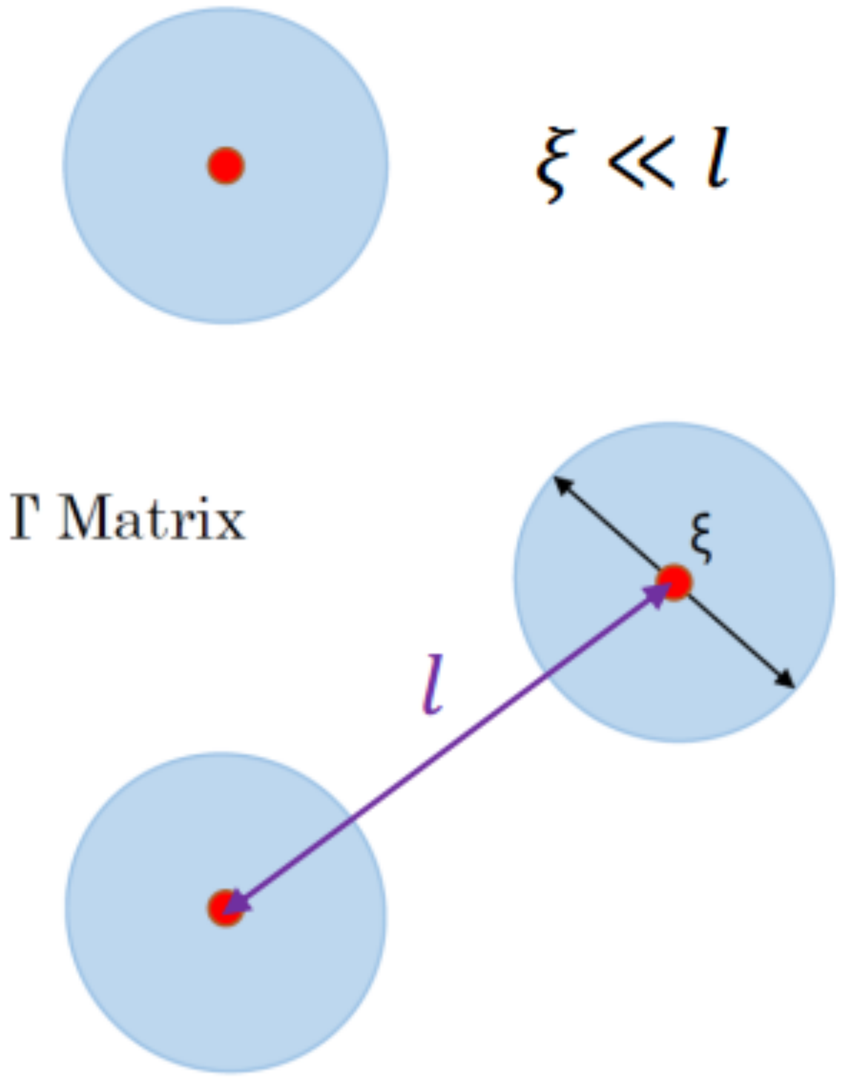

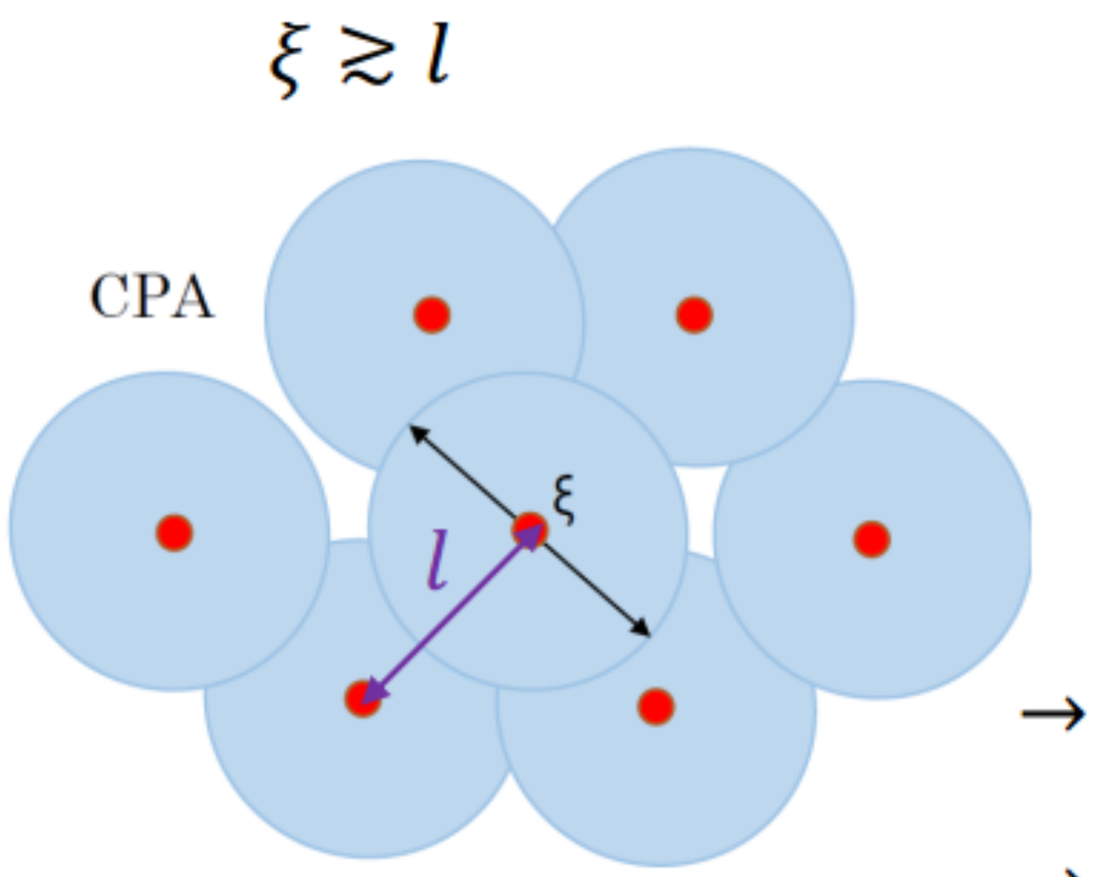

→ *TMA (dilute gas of impurities)*

→ *bound state within the gap*

→ *spatialy fluctuating* $N(\omega)$

→ *CPA (dense gas of impurities)*

→ *overlaping bound states within the gap*

→ *multisite scattering considered*

→ *homogeneous* $N(\omega)$ *(experimentaly required)*

Green function + CPA

- Main object: *Nambu-Gorkov averaged Green's function* $\hat{G}_M$, defined by: $\hat{G}_M^{-1} = \hat{G}_0^{-1} - \hat{\Sigma}$.

i) $\hat{G}_0^{-1}(\mathbf{k}, \omega_n) = i\omega_n\tau_0 - \varepsilon_{\mathbf{k}}\tau_3$: the bare Green's function.

ω_n: Matsubara frequencies, τ_i: Pauli matrices.

ii) $\hat{\Sigma}_n = i\omega_n(1 - Z_n)\tau_0 + Z_n\Delta_n\tau_1$: *Self-energy* generated by disorder and pairing interactions. Functions Δ_n and Z_n contain complete information about the properties of the considered superconductor.

- CPA equations:

$$\hat{\mathcal{G}}_n = \left\langle \left(\hat{\mathcal{G}}_n^{-1} - \hat{V} + \hat{\Sigma}_n \right)^{-1} \right\rangle$$

Impurity potential: $\hat{V} = \bar{\Delta}\tau_1 + U\tau_3 + V\tau_0$.

The index ii denotes the diagonal component (in coordinate space) of a matrix and $\langle f(U,V)\rangle = \int dU \int dV P_s(U)P_m(V)f(U,V)$.

Dynes Superconductor
Model

- Hamiltonian:

$$H = H_0 + \sum_i \bar{\Delta} \left(c_{i\downarrow} c_{i\uparrow} + h.c. \right) + \sum_{i,\sigma} \left(U_i c_{i\sigma}^{+} c_{i\sigma} + V_i \sigma c_{i\sigma}^{+} c_{i\sigma} \right)$$

H_0: free electrons.
$\bar{\Delta}$: spatially homogeneous pairing interaction.
U: pair-conserving fluctuating field.
V: pair-breaking fluctuating field with fixed polarization in spin space.

- $P_s(U)$ and $P_m(V)$: Uncorrelated and even distributions of potential (U) and magnetic (V) impurities.

Dynes Superconductor

From the bullet train

- Generalization of the BCS superconductor including pair-breaking and pair-conserving scattering processes (smearing of all undesired infinities)

- Mathematical formulation using Green function method:

$$\hat{G}(\mathbf{k}, \omega) = \frac{1}{2}\delta \ln \left[\varepsilon_{\mathbf{k}}^2 - \epsilon(\omega)^2\right],$$

$$\delta = \tau_0\partial_\omega - \tau_1\partial_\Delta - \tau_3\partial_{\varepsilon_{\mathbf{k}}},$$

$$\epsilon(\omega) = \sqrt{(\omega + i\Gamma)^2 - \Delta^2} + i\Gamma_s.$$

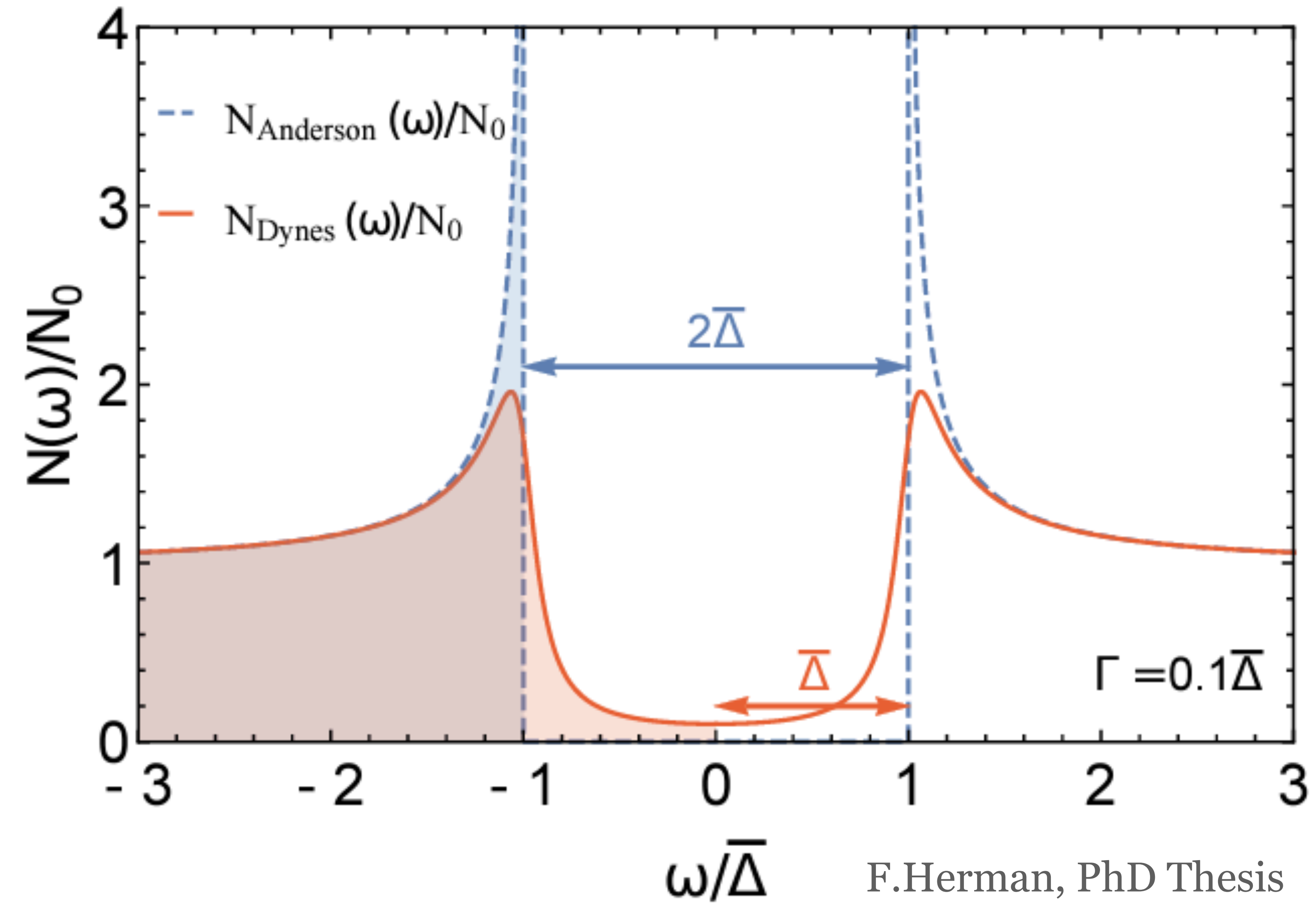

F.Herman, PhD Thesis

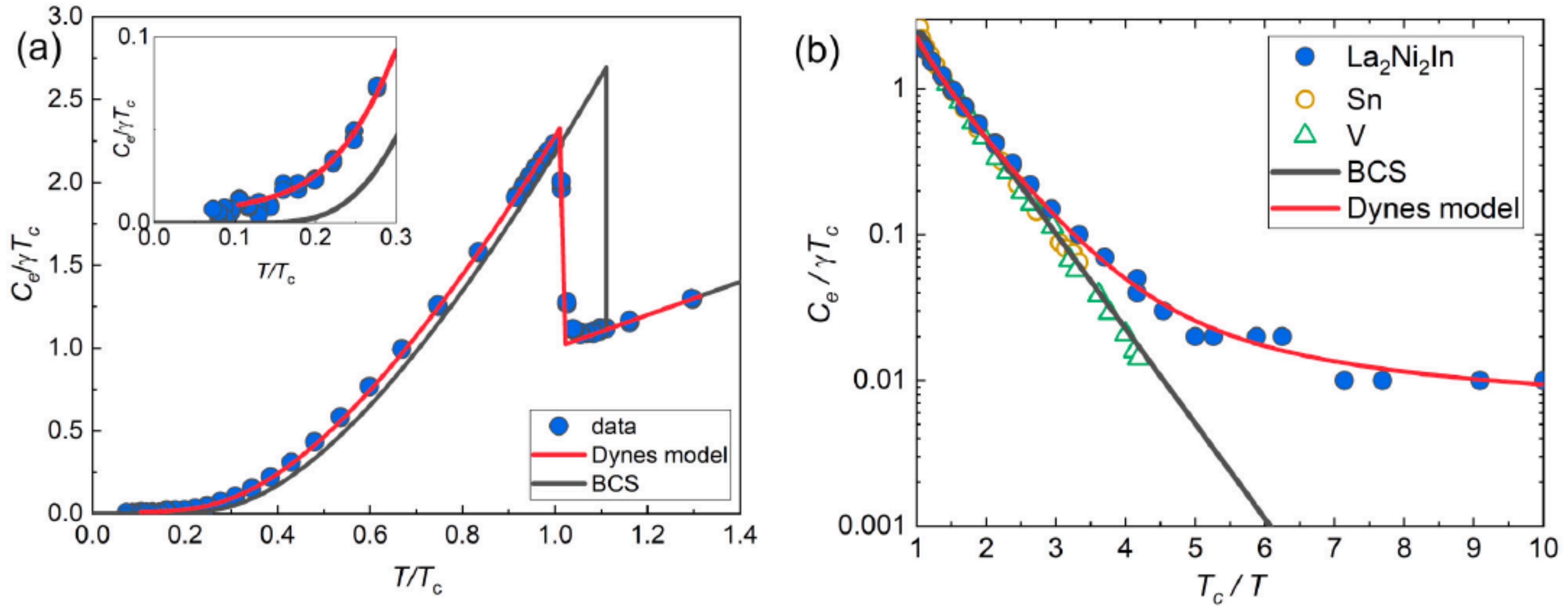

Maiwald et al., PRB **102**, 165125 (2020)

Dynes Superconductor

Electromagnetic properties and optical conductivity

Electromagnetic properties of impure superconductors with pair-breaking processes

František Herman and Richard Hlubina

Phys. Rev. B **96**, 014509 – Published 12 July 2017

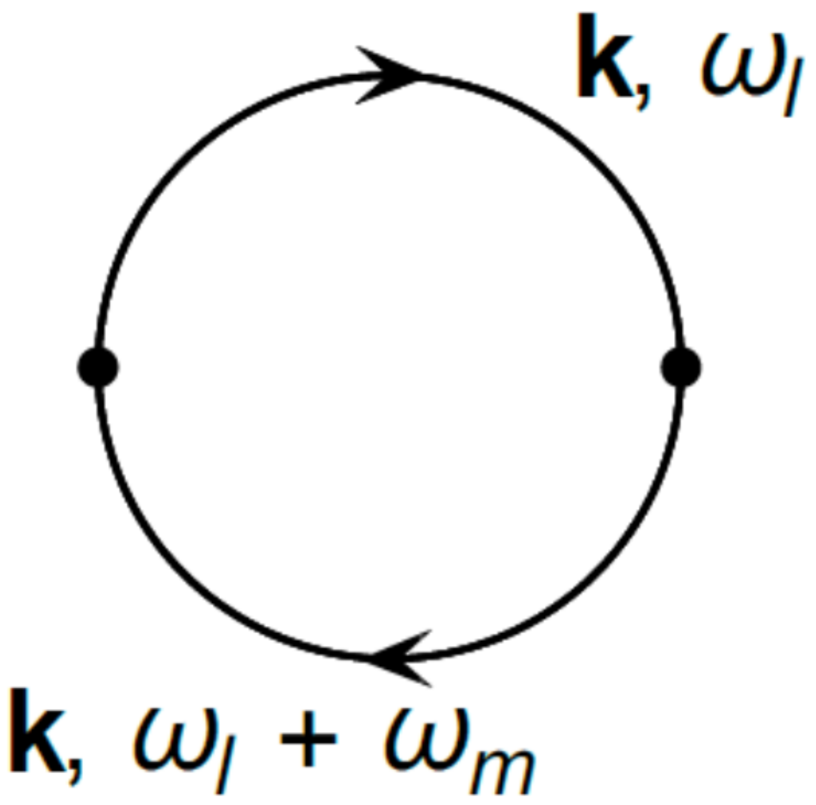

$$\sigma(\omega) = \frac{i}{\omega + i0^+} K(\omega),$$

$$K(\omega_m) \quad = \quad D_0 + \frac{e^2 v_F^2}{3} \int \frac{d^3\mathbf{k}}{(2\pi)^3} T \sum_{\omega_l} \mathrm{Tr}\left[\hat{G}(\mathbf{k}, \omega_l + \omega_m)\hat{G}(\mathbf{k}, \omega_l)\right]$$

diamagnetic part *paramagnetic part*

Dynes Superconductor

Electromagnetic properties and optical conductivity

Phys. Rev. B **96**, 014509

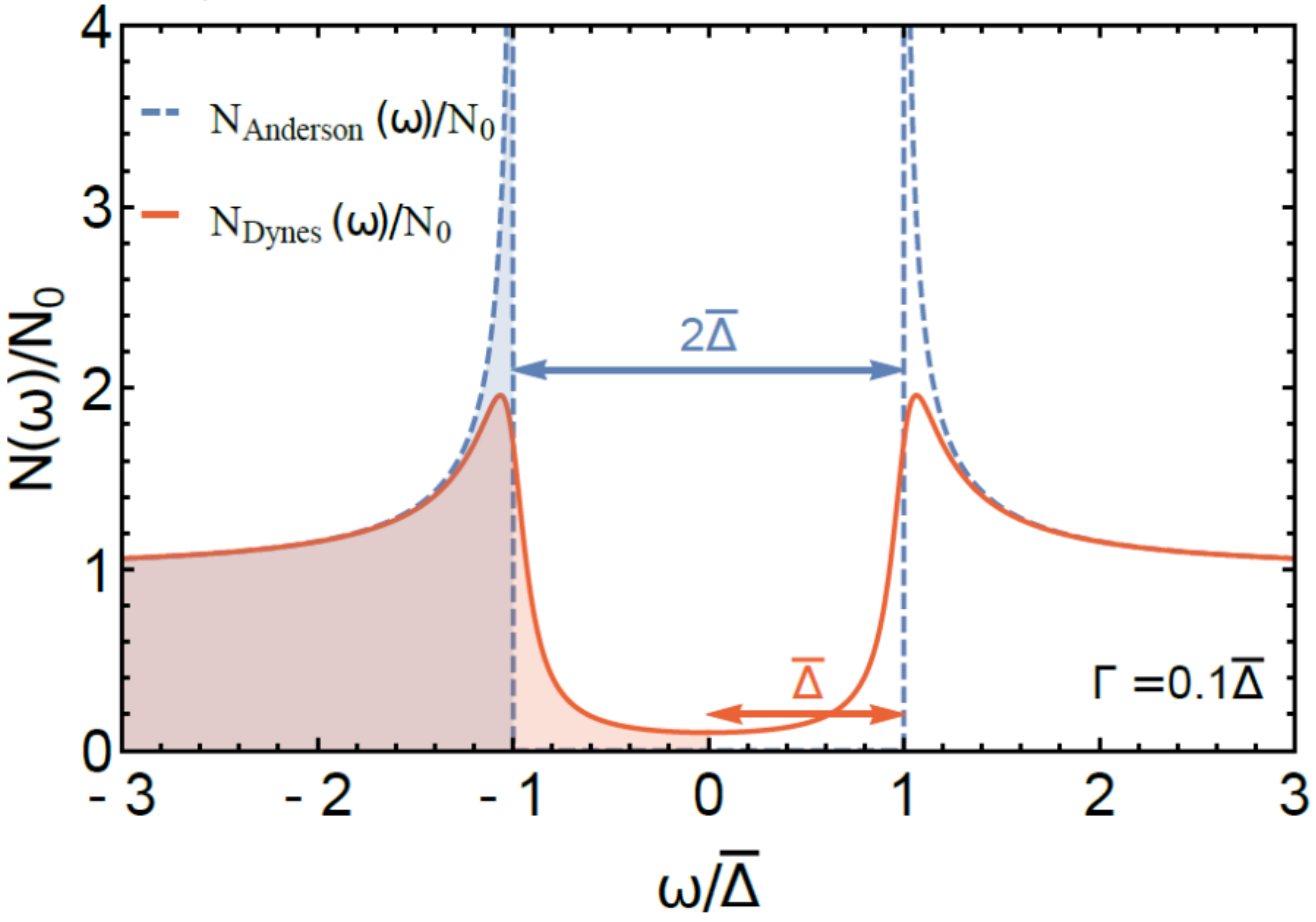

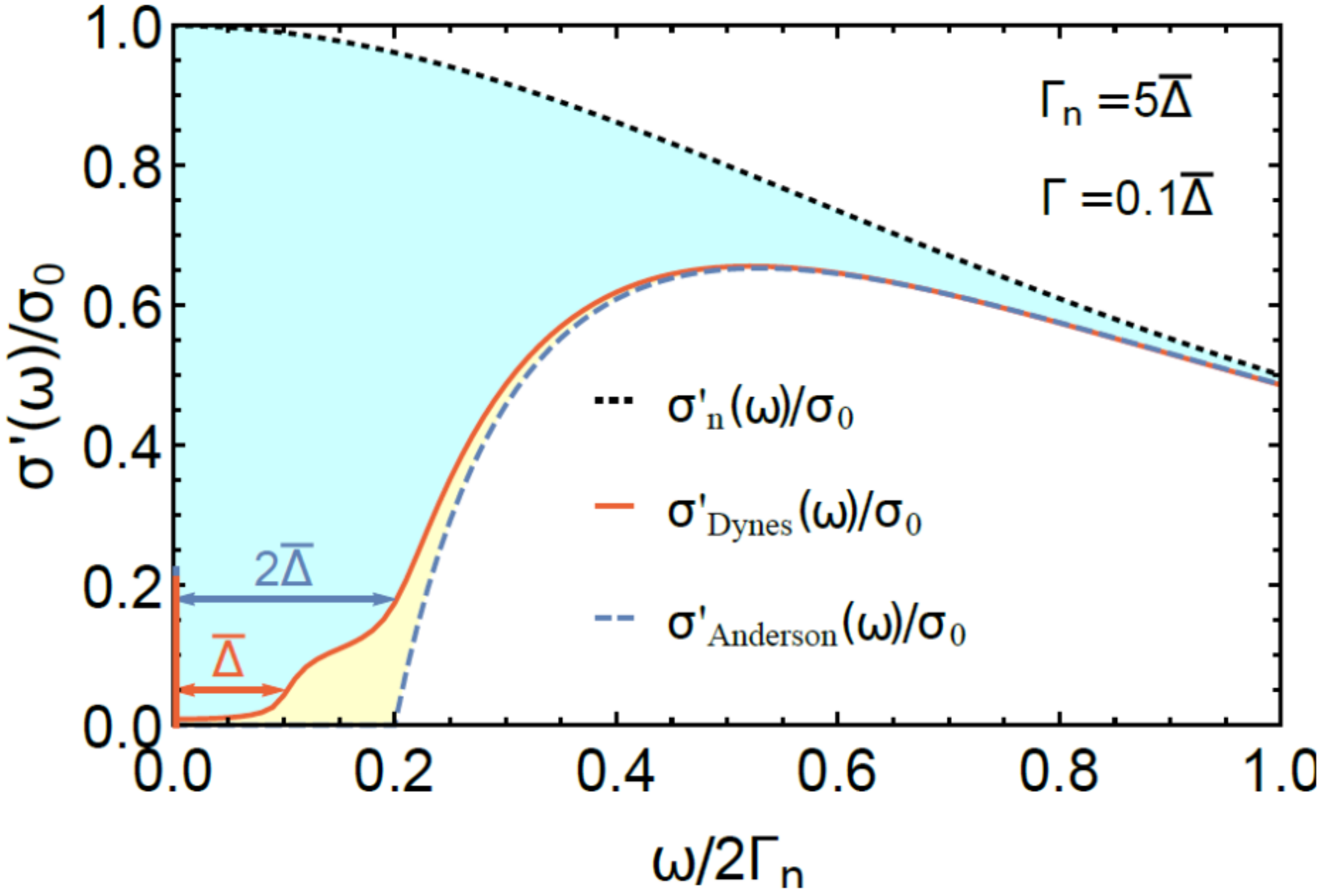

→ *Optical Conductivity*: $\sigma(\omega) = \pi D \delta(\omega) + \sigma_{reg}(\omega)$

→ *Two absorption edges at* $\omega = \bar{\Delta}$ *and* $\omega = 2\bar{\Delta}$

→ *sum rule*: $\int_0^\infty d\omega\, \sigma'(\omega) = \pi/2$

→ $\sigma'_{reg}(\omega)$ *finite down to* $\omega \to 0$ *and* $T \to 0$

Dynes Superconductor

Electromagnetic properties and optical conductivity

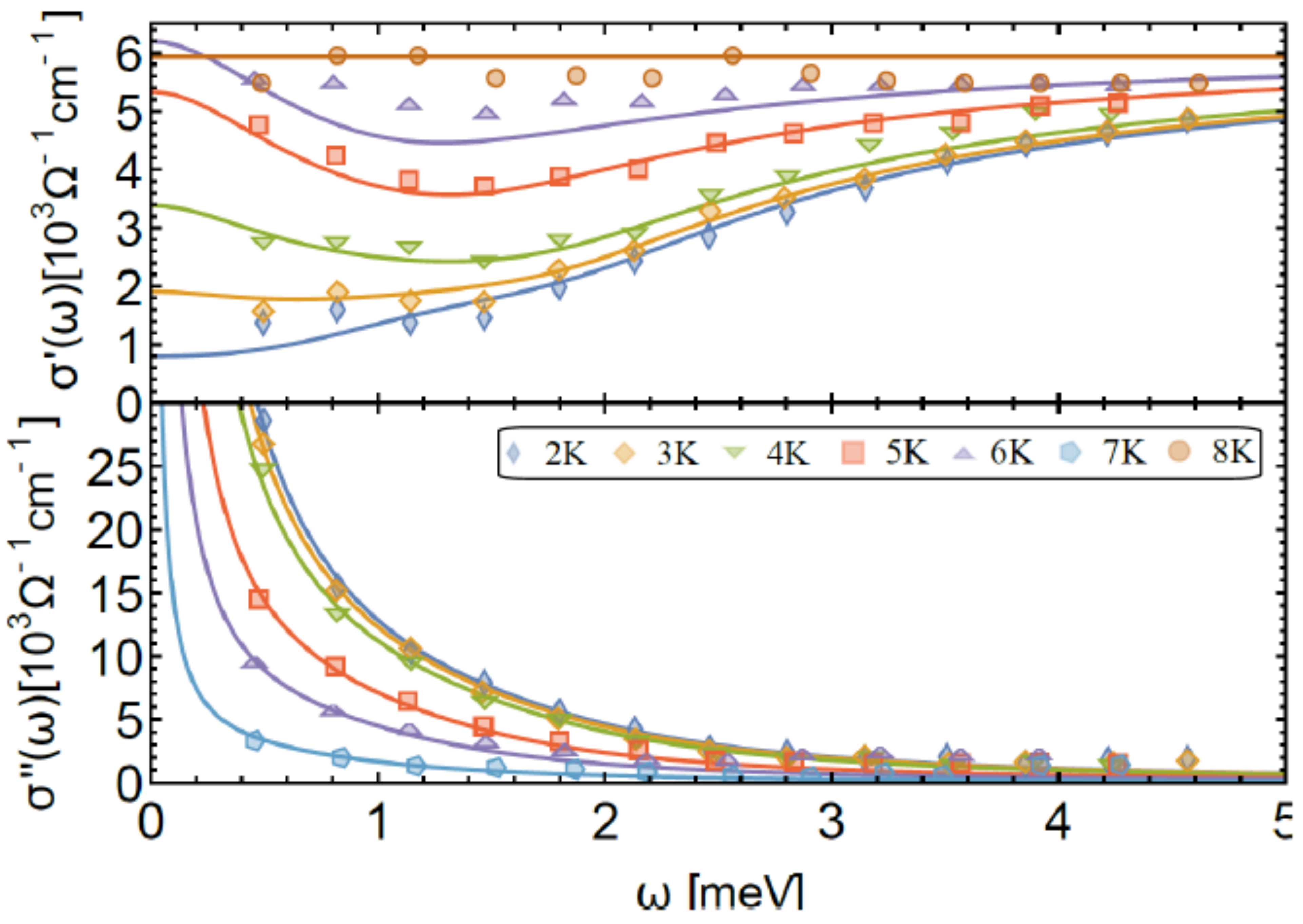

J. Simmendinger *et* al., PRB **94**, 064506 (2016)

$\rightarrow T = 2K: 3\ parameters\ \{\sigma_0, \bar{\Delta}(T), \Gamma\}$

$\rightarrow T > 2K: 1\ parameter\ \{\bar{\Delta}(T)\}$

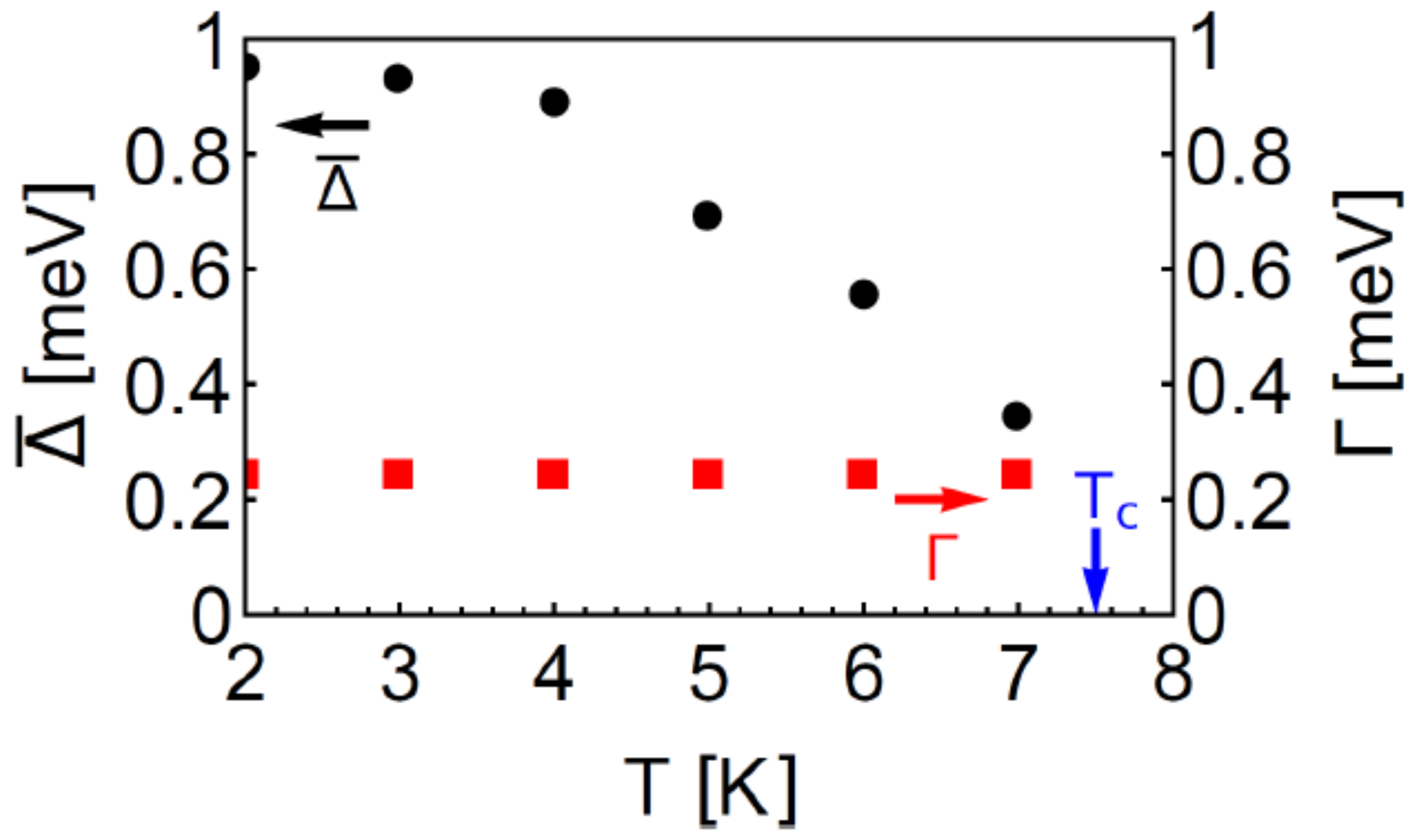

Phys. Rev. B **96**, 014509

Dynes Superconductor

Implications towards the superconductive cavities: **Coherence peak**

Microwave response of superconductors that obey local electrodynamics

František Herman and Richard Hlubina

Phys. Rev. B **104**, 094519 – Published 21 September 2021

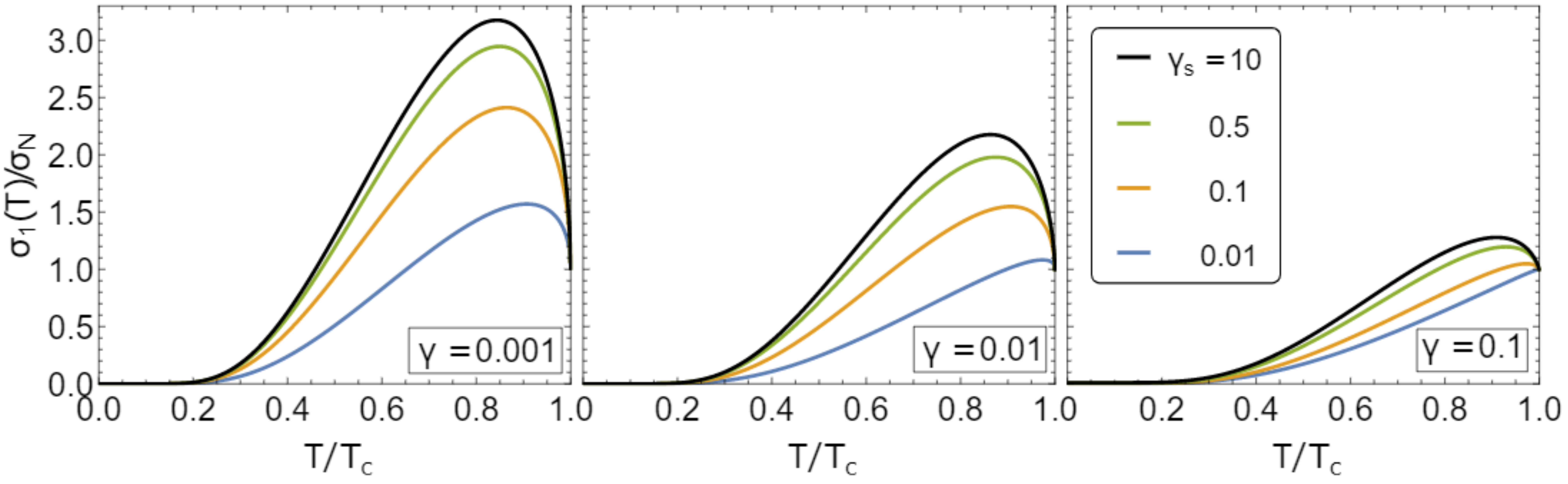

FIG. 1. Temperature dependence of the $\omega \to 0$ limit of $\sigma_1(T)/\sigma_N$ as a function of T/T_c for several values of γ and γ_s. Note that the same peak height can be reached for different combinations of γ and γ_s.

Dynes Superconductor

Implications towards the superconductive cavities: **Coherence peak**

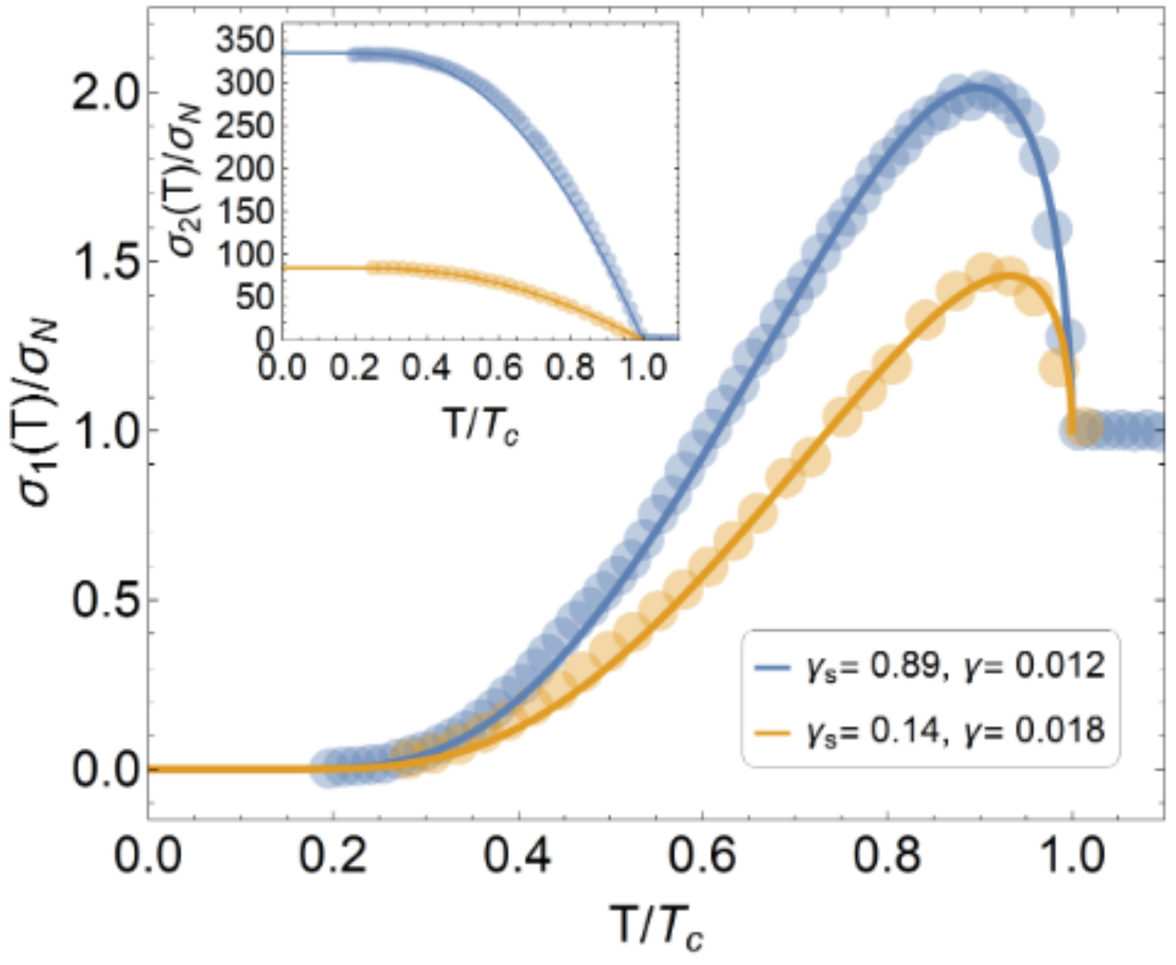

FIG. 9. Real and imaginary parts of the conductivities of the two samples from Fig. 4 in [13] (symbols), together with their fits by the theory of Dynes superconductors with the strong-coupling corrections described for both samples by $x = 1.145$ (lines).

D. Bafia et al., ArXiv:2106.10601 (2021)

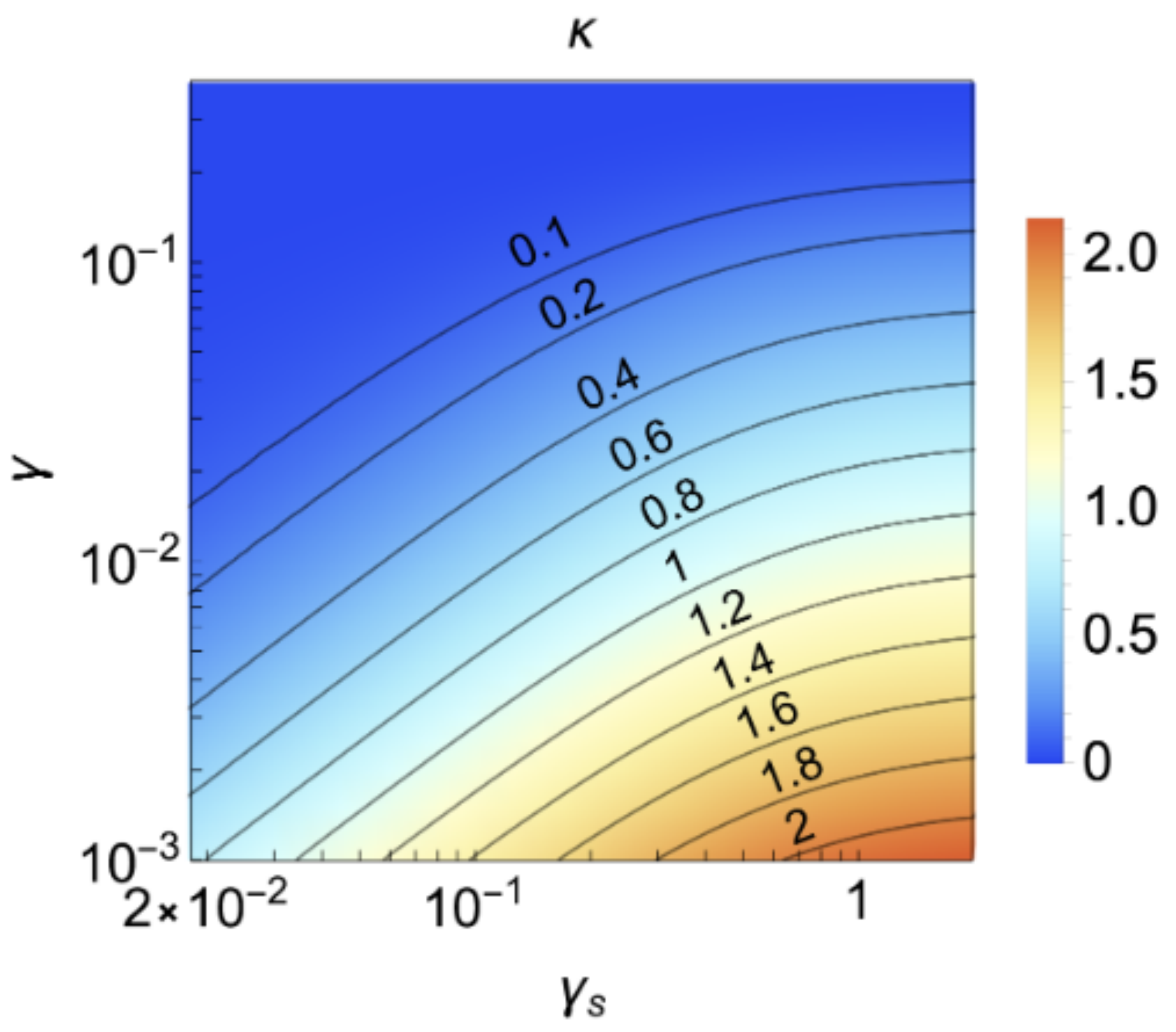

FIG. 2. Height of the coherence peak $\kappa = \sigma_{1,\max}/\sigma_N - 1$ (magnitude indicated by the black labels) as a function of the dimensionless scattering rates γ_s and γ.

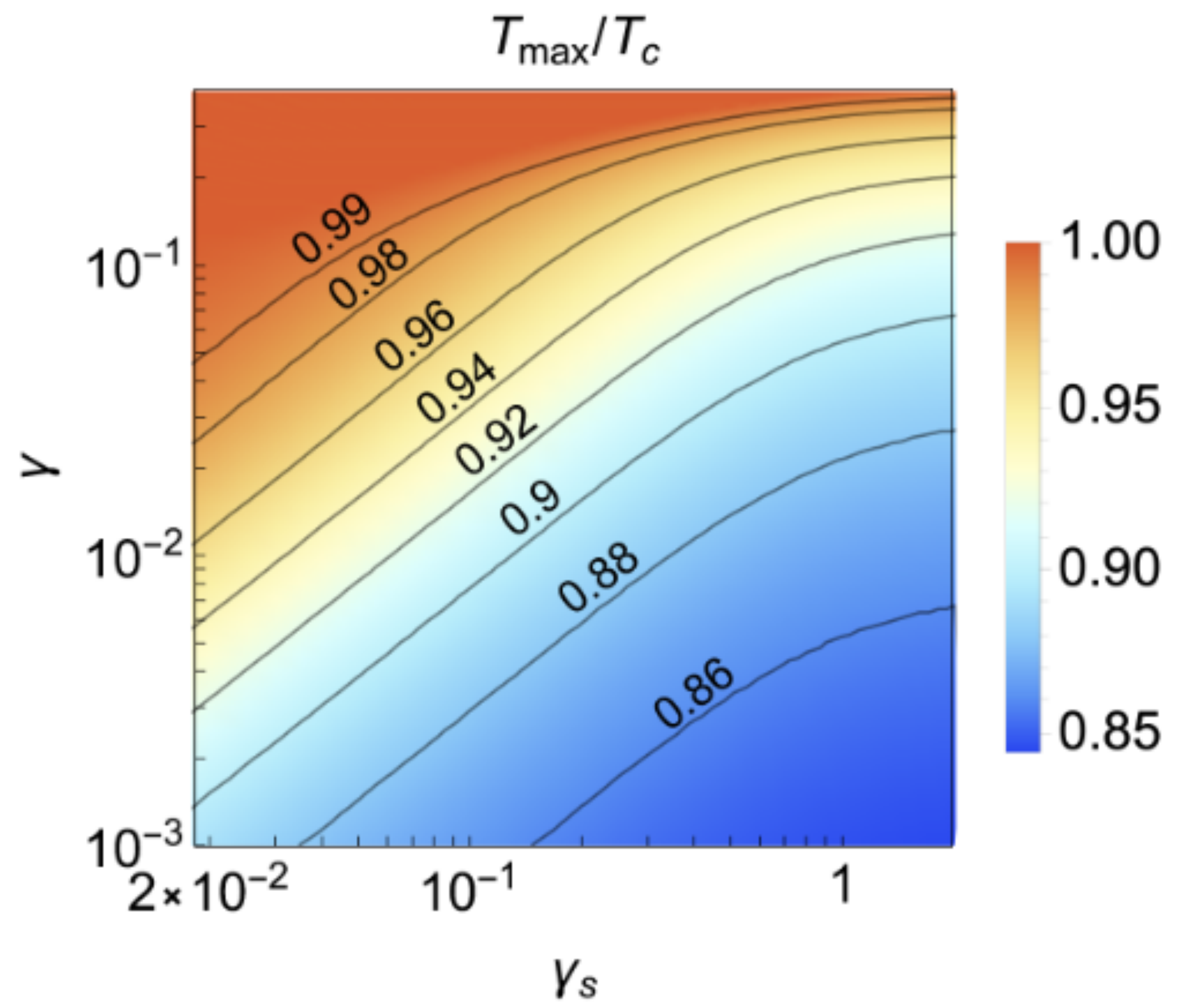

FIG. 4. Position $T_{\max}/T_c$ (indicated by the black labels) of the coherence peak of σ_1/σ_N as a function of γ_s and γ.

Phys. Rev. B **104**, 094519

Research going in similar direction

If not the same

Condensed Matter > Superconductivity

[Submitted on 1 Oct 2021]

Effects of nonmagnetic impurities and subgap states on the kinetic inductance, complex conductivity, quality factor and depairing current density

Takayuki Kubo

We investigate how a combination of a nonmagnetic-impurity scattering rate γ and finite subgap states parametrized by Dynes Γ affects various physical quantities relevant to to superconducting devices: kinetic inductance L_k, complex conductivity σ, surface resistance R_s, quality factor Q, and depairing current density J_d. All the calculations are based on the Eilenberger formalism of the BCS theory. We assume the device materials are extreme type-II s-wave superconductors. It is well known that the optimum impurity concentration ($\gamma/\Delta_0 \sim 1$) minimizes R_s. Here, Δ_0 is the pair potential for the idealized ($\Gamma \to 0$) superconductor for the temperature $T \to 0$. We find the optimum Γ can also reduce R_s by one order of magnitude for a clean superconductor ($\gamma/\Delta_0 < 1$) and a few tens % for a dirty superconductor ($\gamma/\Delta_0 > 1$). Also, we find a nearly-ideal ($\Gamma/\Delta_0 \ll 1$) clean-limit superconductor exhibits a frequency-independent R_s for a broad range of frequency ω, which can significantly improve Q of a very compact cavity with a few tens of GHz frequency. As Γ or γ increases, the plateau disappears, and R_s obeys the ω^2 dependence. The subgap-state-induced residual surface resistance $R_{\rm res}$ is also studied, which can be detected by an SRF-grade high-Q 3D resonator. We calculate $L_k(\gamma, \Gamma, T)$ and $J_d(\gamma, \Gamma, T)$, which are monotonic increasing and decreasing functions of (γ, Γ, T), respectively. Measurements of (γ, Γ) of device materials can give helpful information on engineering (γ, Γ) via materials processing, by which it would be possible to improve Q, engineer L_k, and ameliorate J_d.

Comments: 15 pages, 15 figures

Subjects: **Superconductivity (cond-mat.supr-con)**; Instrumentation and Methods for Astrophysics (astro-ph.IM); Accelerator Physics (physics.acc-ph)

Cite as: arXiv:2110.00573 **[cond-mat.supr-con]**

(or arXiv:2110.00573v1 **[cond-mat.supr-con]** for this version)

Effects of nonmagnetic impurities and subgap states on the <u>kinetic inductance</u>, complex conductivity, quality factor and depairing current density (Kubo, 2021)

- Kinetic inductance

$$\sigma = \frac{ne^2\tau}{m(1+i\omega\tau)} = \frac{ne^2\tau}{m(1+\omega^2\tau^2)} - i\frac{ne^2\omega\tau^2}{m(1+\omega^2\tau^2)}$$

- Superconductor

$$\frac{1}{2}(2m_e v_s^2)(n_s l A) = \frac{1}{2}L_k I^2$$

$$I = 2ev_s n_s A$$

- Important for kinetic inductance detectors (KIDs) and superconductor single-photon detectors (SSPDs)

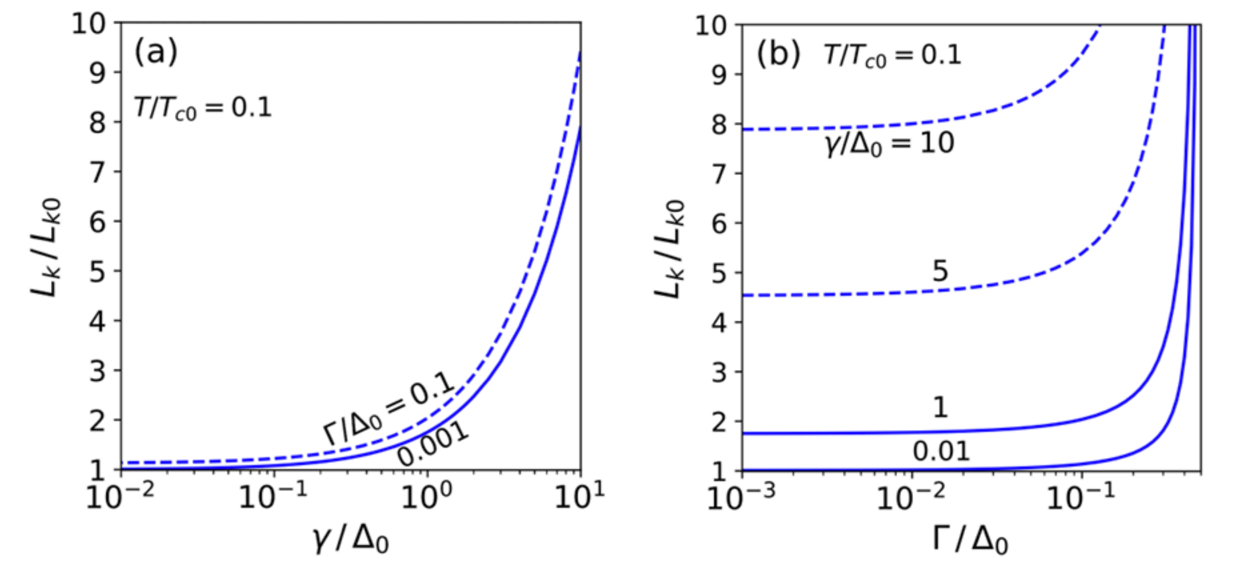

FIG. 4. Kinetic inductivity at $T/T_{c0} = 0.1$ as functions of (a) nonmagnetic-impurity scattering-rate $\gamma/\Delta_0 = \pi\xi_0/2\ell_{imp}$ and (b) Dynes Γ parameter.

Appl. Phys. Lett. **88**, 111116 (2006)

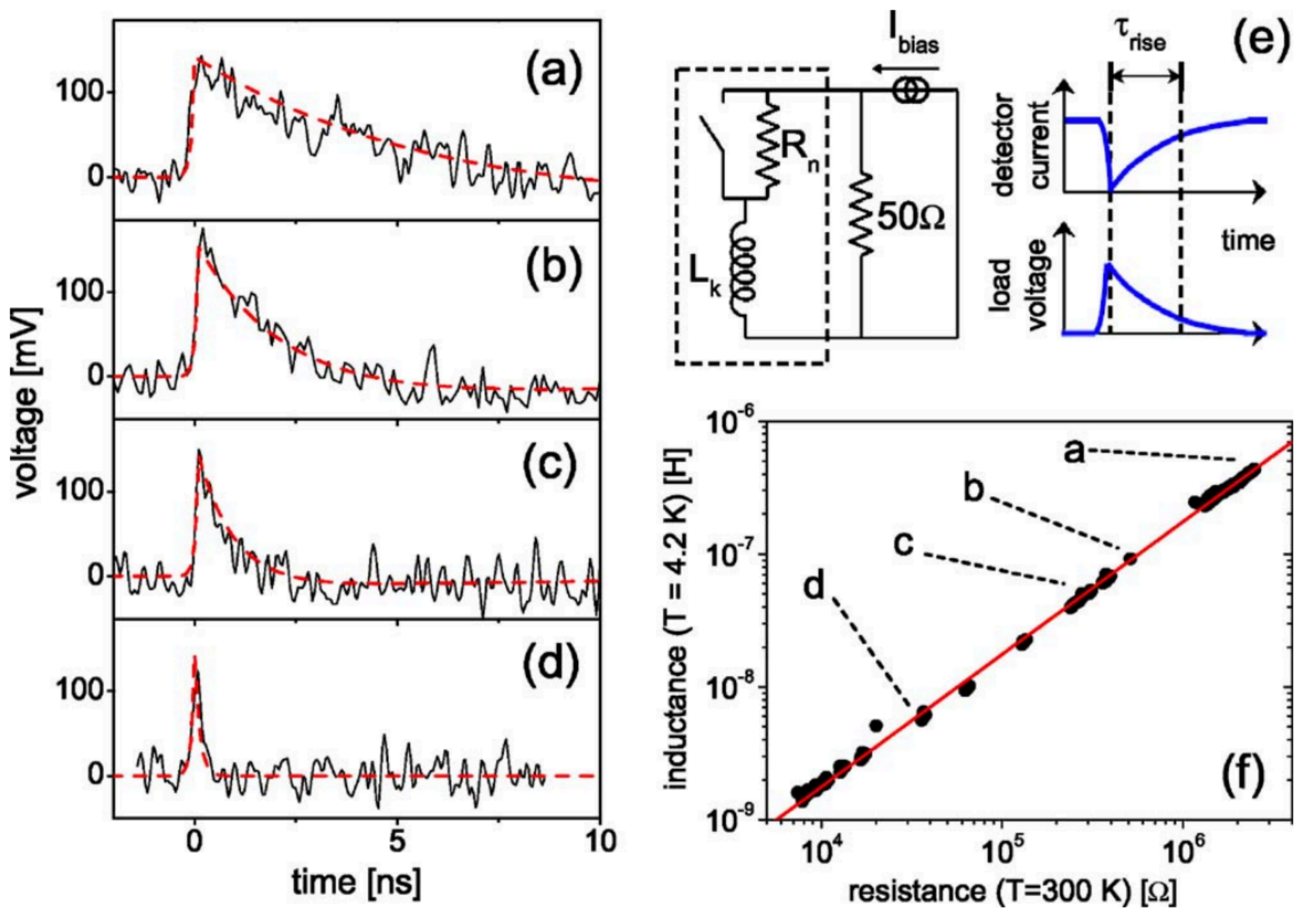

FIG. 2. (Color online) Inductance-limited recovery of NbN nanowires. Output pulses are shown for 100 nm wide wires at T=4.2 K, with I_{bias} =11.5 μA, and dimensions: (a) 10 μm×10 μm meander (total length 500 μm); (b) 4 μm×6 μm (120 μm); (c) 3 μm×3.3 μm (50 μm); and (d) 5 μm long single wire. Red dotted lines show the predicted pulse recovery, with no free parameters, for each device based on its measured inductance: L_k=415 nH, 110 nH, 44.5 nH, and 6.10 nH. These predictions include the effect of the measured f_L=15 MHz and f_H=4 GHz corner frequencies of our amplifiers, and the assumptions: $I_{ret} \ll I_{bias}$, $R_n \gg 2\pi f_H L_k$, and $R_n \gg 50\ \Omega$ (the pulse risetime is then determined by f_H); and (e) electrical model; photon absorption corresponds to the switch opening, after which the detector current goes nearly to zero, and is diverted into the 50 Ω load. The wire then becomes superconducting again, and the current resets in a time τ_{rise}. (f) Inductance at T=4.2 K vs room-temperature resistance for 290 individual nanowires from 0.5–500 μm long and 20–400 nm wide, with both straight and meander geometries, from two separate samples made in separate fabrication runs. Points corresponding to the devices of (a)–(d)

Effects of nonmagnetic impurities and subgap states on the kinetic inductance, complex conductivity, <u>quality factor</u> and depairing current density (Kubo, 2021)

- Surface resistance

$$R_s = \frac{1}{2}\mu_0^2\omega^2\lambda^3\sigma_1$$

- Quality

$$Q = \frac{G}{R_s}, \qquad G = \frac{\mu_0\omega \int |\mathbf{H}|^2 dV}{\int |\mathbf{H}|^2 dS}$$

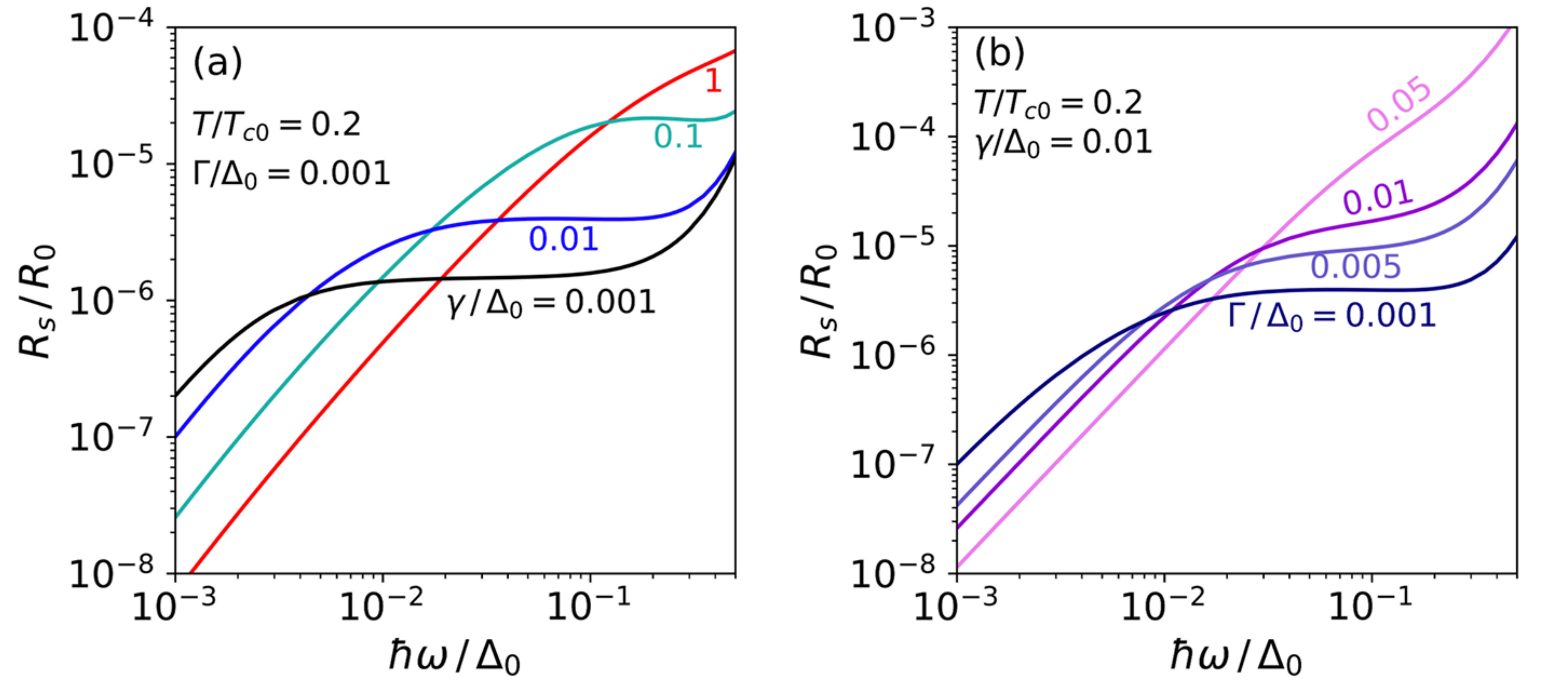

FIG. 10. Frequency dependences of the surface resistance R_s (a) calculated for different nonmagnetic-impurity scattering rate γ and (b) calculated for different Dynes Γ.

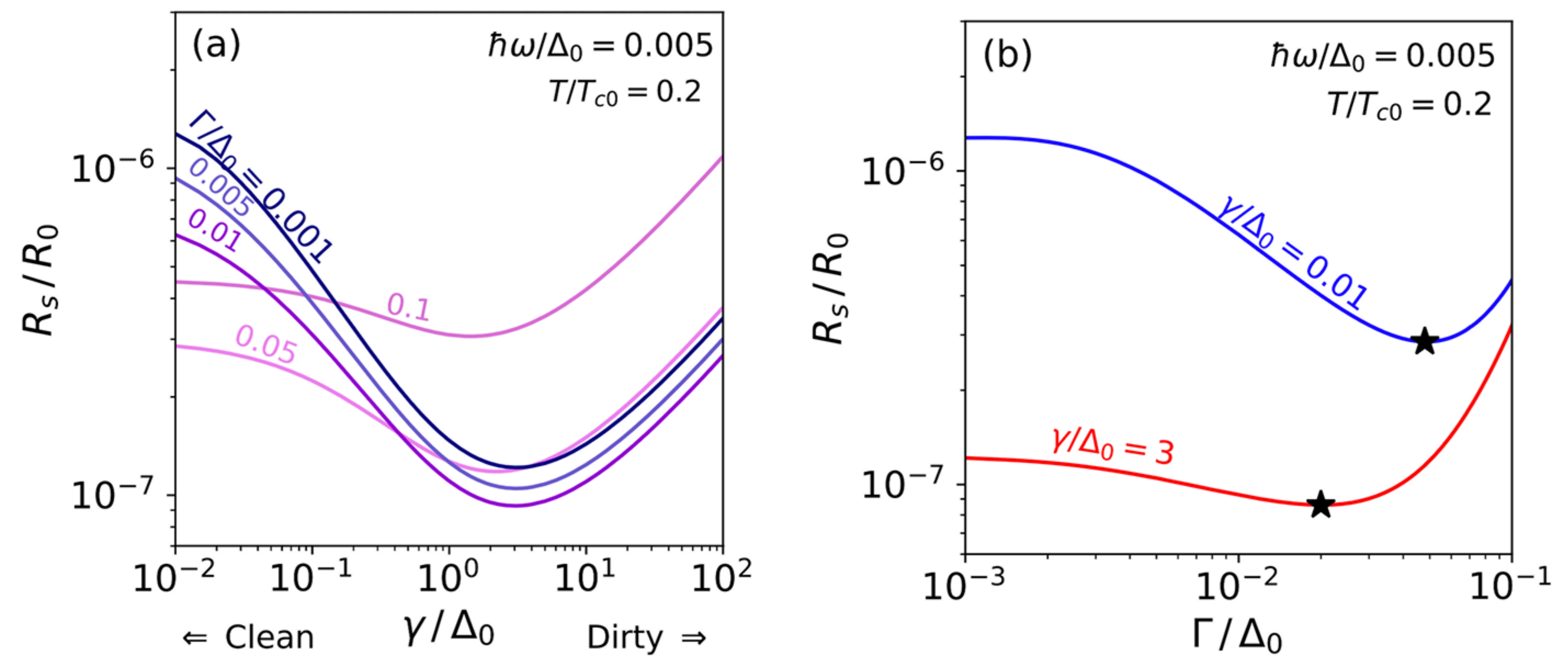

FIG. 11. (a) R_s as functions of nonmagnetic-impurity scattering-rate $\gamma/\Delta_0 = \pi\xi_0/2\ell_{\rm imp}$ calculated for different Γ. (b) R_s as functions of Γ calculated for $\gamma/\Delta_0 = 3$ (red) and $\gamma/\Delta_0 = 0.01$ (blue). The black stars are the minimums.